Accepted Manuscript

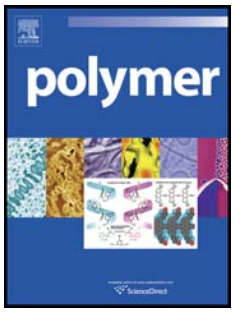

A general method for functionalisation of microgel particles with primary amines using click chemistry

Robert Farley, Brian R. Saunders

PII: S0032-3861(13)01122-1

DOI: 10.1016/j.polymer.2013.12.022

Reference: JPOL 16659

To appear in: *Polymer*

Received Date: 27 October 2013

Revised Date: 7 December 2013

Accepted Date: 10 December 2013

Please cite this article as: Farley R, Saunders BR, A general method for functionalisation of microgel particles with primary amines using click chemistry, *Polymer* (2014), doi: 10.1016/j.polymer.2013.12.022.

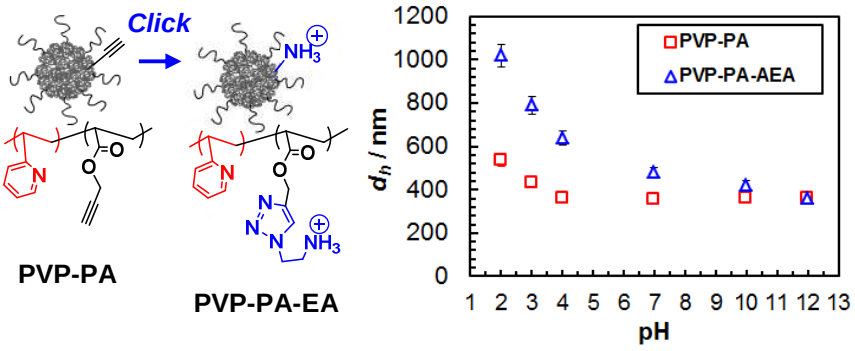
Click
NH3
O
N
N
N
N
NH3
PVP-PA
PVP-PA-EA
1200
1000
800
600
400
200
0
dh / nm
1 2 3 4 5 6 7 8 9 10 11 12 13
pH
PVP-PA
PVP-PA-AEA

A general method for functionalisation of microgel particles with primary amines using click chemistry

Robert Farley[a] and Brian R. Saunders[a,]*

[a]*Biomaterials Research Group, Manchester Materials Science Centre, School of Materials, The University of Manchester, Grosvenor Street, Manchester, M1 7HS, U.K.*

ABSTRACT

In this study we introduce a general method for functionalising microgel particles with primary amine groups using a one-step copper catalysed azide-alkyne cycloaddition (CuAAC) reaction. Three different families of microgels containing copolymerised propargyl acrylate (PA) were prepared and then reacted with 2-azido-1-ethylamine (AEA) using CuAAC. The microgels contained poly(ethyl acrylate) (PEA), poly(2-vinylpyridine) (PVP) or poly(*N*-isopropylacrylamide) (PNP). The functionalisation of the microgels containing PA (i.e., PX-PA) by AEA to give primary amine functionalised particles (PX-PA-AEA) was assessed by elemental analysis and FTIR. The reaction of AEA with PA was quantitative for each of the PX-PA-AEA microgels (X = EA, VP and NP). The PX-PA-AEA systems generally showed larger pH-triggered swelling and zeta potentials than the non-clicked PX-PA particles. The results also showed that PA restricted swelling of the PX-PA and PX-PA-AEA particles by acting as a crosslinker. Of the three microgel systems studied, PVP-PA-AEA had the best combination of high AEA incorporation and pH-triggered swelling.

* Brian.saunders@manchester.ac.uk, Tel: 44 161 306 5944

INTRODUCTION

The long-standing interest in microgels in the literature continues to increase[1-4]. Microgels are crosslinked polymer colloids that swell in a good solvent or when the pH approaches the pK_a of the polyacid or polybase chains from which they are composed. Microgels can be designed to be thermally responsive[5-9], pH-responsive[10, 11] or light responsive[12]. They have excellent potential for construction of advanced responsive materials and biomaterials[13]. However, the preparation of future advanced materials from microgels requires new methods for functionalising the particles in a controlled manner. Ideally, functionalisation should occur quantitatively and without sacrificing colloidal stability of the dispersions. Of special interest is the challenge of preparing microgel particles containing high concentrations of primary amines. Microgels containing high primary amine contents would themselves provide useful building blocks for construction of complex assemblies because of the versatile nature of primary amine reactions[14]. Unfortunately, microgels containing high primary amine contents have been challenging to prepare as stable dispersions[15]. Copper catalysed azide-alkyne cycloaddition (CuAAC)[16, 17] has proven to be a very effective functionalisation method for polymers and nanoparticles. CuAAC has high efficiency, high tolerance to functional groups and solvents, requires moderate reaction temperatures and is effective for a range of interfaces[18-21]. The reaction yields little or no by-products. We were inspired by the work of Jung et al.[22] which showed that it was possible functionalise linear alkyne-containing polymers with primary amines using CuAAC. Here, we sought to establish a general method that would allow a range of alkyne-containing microgels to be functionalised with an azide-functionalised primary amine in one step. In doing so we test the general principle that CuAAC reactions provide quantitative reaction for a range of interfaces[20]. In the present case the interfaces consist of swollen polymer chains within microgel particles. In addition to demonstrating the generality of CuAAC reactions for three different microgel types, this study establishes a new general method for preparing microgels functionalised with primary amines.

CuAAC has been successfully used to prepare a wide range of materials with precise design requirements. Budhathoki-Uprety used CuAAC to construct perfectly alternating functional polymers[23]. CuAAc has been used to prepare new functional monomers[24], functionalise surfaces[25] and construct novel delivery systems[26]. CuAAC is a spring-loaded reaction[27] that is well suited to nanoparticle functionalisation[28]. Gokmen et al.[29] demonstrated post-functionalisation of polymerised high-internal phase emulsion beads using CuAAC. A key aspect for the success of the reaction in the later study was good accessibility to the grafted azide groups by the alkyne-based chromophore. CuAAC has also been studied in the context of core-shell PS particles[30]. The latter were prepared with an uncrosslinked poly(methyl methacrylate-*co*-propargyl acrylate) shell and functionalised with azide-terminated PEGs. That study noted that high levels of propargyl acrylate (PA) could cause shell crosslinking. Evanoff et al. prepared poly(PA) particles by emulsion polymerisation and used CuAAC to functionalise crystalline colloidal arrays[31]. CuAAC has also been used to functionalise shell-crosslinked nanoparticles[32].

CuAAC offers excellent potential to functionalise microgels by bespoke placement of azide or alkyne groups. However, there have been very few publications involving CuAAC for microgels. In a seminal study Meng et al.[33] copolymerised PA within the shell of poly(*N*-isopropylacrylamide-*co*-acrylic acid) (PNP-AA) microgels and then functionalised the microgels with azide dyes. The level of PA incorporated within those microgel particles was low (nominal PA content was 5 mol.% based on monomer) and the PA was confined to the shells because a seed-feed preparation method was used. Kupal et al.[34] prepared core-shell microgels using assembly of azido and alkyne derivatives of poly(vinyl alcohol). They used residual surface alkyne groups to graft azido-hyaluronic acid and showed that the microgels could target adenocarcinoma colon cells. Here, we employ a PA-based microgel route to prepare three new families of PA-containing microgels. The PA incorporation was between 6.3 and 28 mol.% and is relatively high compared to other work[33].

Scheme 1 shows the PX, PX-PA and PX-PA-AEA systems investigated and their preparation. Here, X = ethylacrylate (EA), 2-vinylpyridine (VP) or *N*-isopropylacrylamide (NP). The poly(ethyl

acrylate)/PA microgel (PEA-PA) was not intrinsically pH-responsive. PEA is hydrophobic and the linear polymer has a glass transition temperature of about -24 ^{o}C[35]. The poly(2-vinylpyridine)/PA (PVP-PA) microgel is pH-responsive. Linear PVP is a weak polybase and is soluble in the protonated form at pH values greater than about 4.0[36]. The poly(*N*-isopropylacrylamide)/PA (PNP-PA) microgel was temperature-responsive and PNP has a lower critical solution temperature of about 32 ^{o}C[37]. Those particles were mostly hydrophilic at room temperature. Consequently, the three families of microgels have very different swelling behaviours. However, they were all prepared using the same preparation conditions. The crosslinking monomers selected for each microgel (Scheme 1) are well known to provide efficient crosslinking for each system. For the CuAAC reactions, a single (common) method was used which incorporated 2-azido-1-ethylamine (AEA) via the PA groups and formed PX-PA-AEA (Scheme 1).

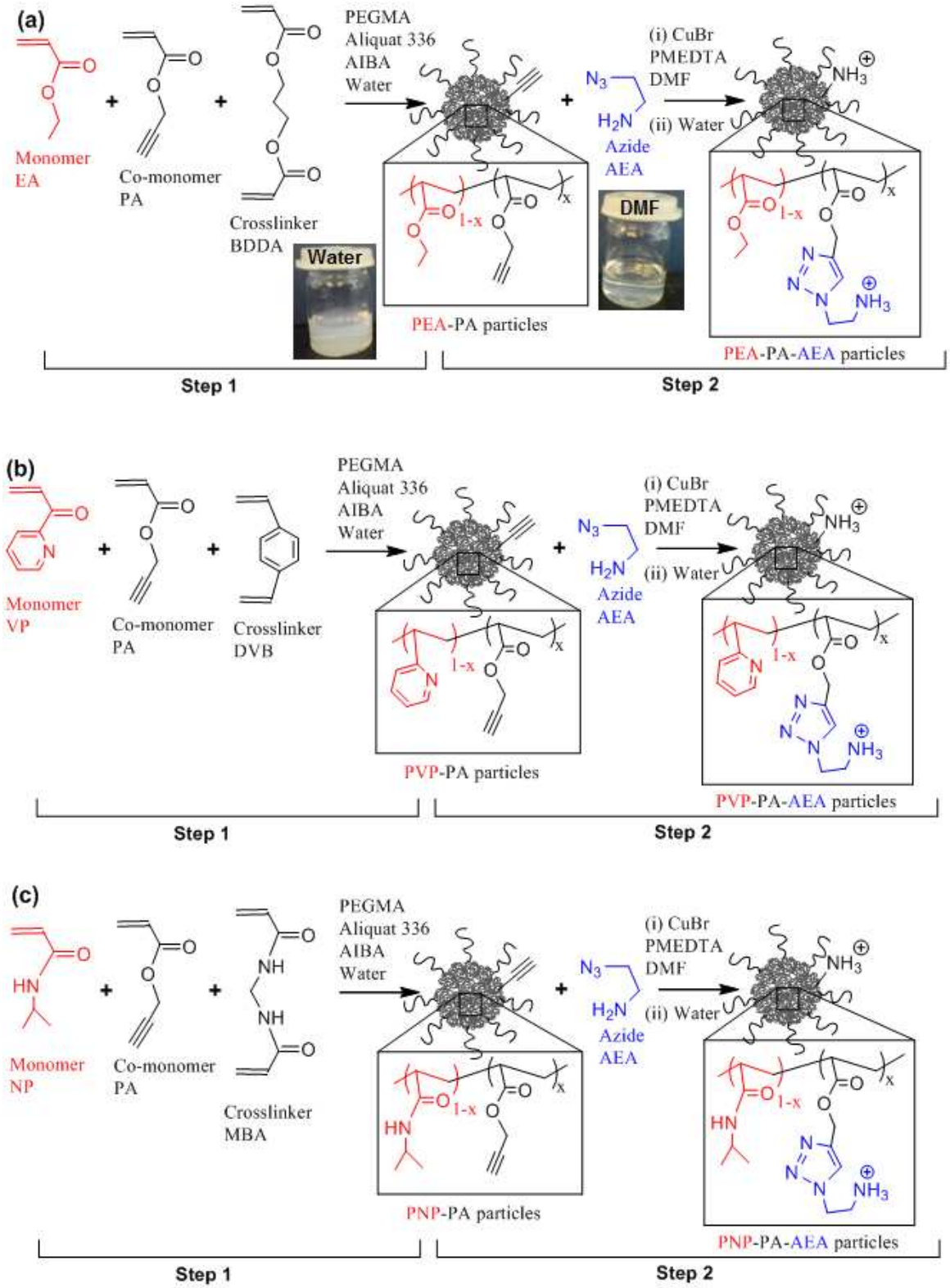

Scheme 1. Preparation of primary amine functionalised microgels using CuAAC chemistry. The tubes in (a) reveal that the turbidity decreased due to microgel particle swelling in DMF. *(Colour reproduction on web, B & W in print.)*

There are several differences for our method for CuAAC of microgels compared to other reports[33]. Firstly, the PX-PA microgels were prepared in a single step. Furthermore, in contrast to the

approach by Meng et al.[33] we used a solvent exchange method (via centrifugation) to transfer the particles from water to DMF for the CuAAC reaction (Scheme 1). The PX-PA-AEA particles were then dialysed against water to transfer them back to that phase. This process prevented the particles becoming dry at any stage and preserved dispersion stability. PEA-PA and PVP-PA as well as all of the PX-PA-AEA microgels have not been reported before to the best of our knowledge.

The study begins with the characterisation and analysis of the compositions of PX (X = EA, VP and NP), PX-PA and PX-PA-AEA. We show that incorporation of AEA (and hence primary amines) into the latter was quantitative and determined only by the extent of PA incorporation. The study also investigates the pH-responsive behaviours of the PX-PA-AEA microgels as well as the temperature responsive behaviour of PNP-PA-AEA. It is noted that the PX-PA-AEA systems are well suited to further functionalisation reactions, as shown for other primary amine-rich microgels[15]. This work introduces six microgels (PX-PA and PX-PA-AEA, where X = EA, VP and NP) that have higher PA contents than other microgels[33], were prepared using simple methods and have versatile functionalisation potential.

EXPERIMENTAL

Reagents

EA (99%), NIPAm (97%) and 2VP (97%) were purchased from Aldrich and inhibitor removed by passing chloroform solutions through a neutral alumina column followed by removal of the solvent at reduced pressure. Aliquat 336 and α,α'-azodiisobutyramidine dihydrochloride (AIBA, 97%), 1, 4-butanediol diacrylate (BDD, 90%), *N*-*N*'-methylenebis(acrylamide) (BA, 99%) and *p*-divinylbenzene (DVB, 85%) were also purchased from Aldrich and used as received. Polyethyleneglycol methacrylate (PEGMA) with a number-average molecular weight of 2000 g/mol, NaN_3 (> 99.5%), and 2-chloroethylamine hydrochloride (99%) were purchased from Aldrich and used as received. The following *linear* polymers were purchased from Aldrich and used for solubility tests: poly(2-vinylpyridine) (PVP_L, M_n = 35,000 g/mol, PD = 1.07), poly(ethyl acrylate)

(PEA_L, M_w = 95,000 g/mol) and poly(*N*-isopropylacrylamide) (PNP_L, 19,000 – 30,000 g/mol). For PEA_L, the toluene was removed by rotary evaporation prior to use. High purity water that was distilled and deionised was used.

Synthesis of 2-azido-1-ethylamine

AEA was synthesised according to the method described by Jung et al.[22]. 2-chloroethylamine hydrochloride (5 g, 43 mmol) was ground and dissolved in deionised water (50 ml). Sodium azide (8 g, 123 mmol) was added and the mixture was heated at 80 ^oC for 18 hours. The solution was then made alkaline with potassium hydroxide (15 g), extracted using diethyl ether and dried over magnesium sulphate. Finally the solution was concentrated using rotary evaporation to give an amber coloured, viscous oil. AEA was characterised using ^1H NMR and FTIR spectroscopy (See Fig. S1, Supporting information). The integrations for the peaks gave the correct proton ratios and the FTIR spectra (Fig. 2(a)) showed a strong azide band at 2100 cm^{-1}.

Microgel synthesis

The PX and PX-PA microgels were prepared by a batch emulsion (X = EA and VP) or precipitation (X = NP) process and followed the method of Dupin et al.[10] The masses of the monomers used are given in Table S1. In all cases the mass of PEGMA, Aliquat and AIBA corresponded to, respectively, 10, 1.0 and 1.0 wt.% with respect to the total monomer mass. Briefly, Aliquat 336 (1.50 g) and PEGMA (3.0 g of 50 wt.% aqueous solution) were dissolved in water (120 ml) in a round bottomed flask and the co-monomer mixture added. For example, for preparation of PEA-PA, EA (10.35 g), PA (4.5 g) and BDD (0.15 g) were used. The solution was degassed with argon and then heated with overhead, mechanical, stirring to 60 ^oC. AIBA (0.15 g) was added to begin the polymerisation. This was continued for 24h, after which time the dispersion was extensively dialysed against pH = 3 water. The crosslinking monomers were present at nominal concentration of 1 mol.% with respect to monomer and are not identified in the nomenclature used. Here, PX (X = EA, VP or NP) refer to poly(EA-*co*-BDD), poly(VP-*co*-DVB) or poly(NP-*co*-BA) microgels, respectively. Furthermore, PX-PA (X = EA, VP or NP) refer to poly(EA-*co*-PA-*co*-BDD),

poly(VP-*co*-PA-*co*-DVB) or poly(NP-*co*-PA-*co*-BA) microgels, respectively.

CuAAC Click reaction of microgels with AEA

The PX-PA microgel (0.2 g of particles) was transferred to DMF from water using centrifugation and re-dispersion. The number of moles of PA present was typically 0.55 mmole. After degassing the dispersion thoroughly, AEA (0.163 g, 1.33 mmole), *N,N,N′,N″,N″*-pentamethyldiethylenetriamine (PMDETA, 0.0165 g, 0.095 mmole) and CuBr (0.0136 g, 0.095 mmole) were added with stirring. The dispersion remained colloidally stable and the reaction was allowed to proceed for 24 h at room temperature. The product was then extensively dialysed against pH = 3 water to replace the DMF solvent with water. PX-PA-AEA (X = EA, VP or NP) refer to poly(EA-*co*-(PA-AEA)-*co*-BDD), poly(VP-*co*-(PA-AEA)-*co*-DVB) or poly(NP-*co*-(PA-AEA)-*co*-BA) microgels, respectively.

Physical Measurements

Elemental analysis (C, H, and N) was performed at the School of Chemistry, University of Manchester using a Thermo Scientific Flash 2000 Organic Elemental Analyzer with the calibration standards acetanilide and cyclohexanone 2,4 dinitrophenylhydrazone. The samples were freeze-dried prior to measurement and the data are from single measurements. We have found elemental analysis to be a very reproducible technique and the errors estimated from multiple analysis of related polymers within our group are shown in Table S2. Fourier transform infrared (FTIR) measurements were conducted on a Nicolet 5700 ATR FTIR instrument. Microgel samples were freeze-dried to allow analysis, while PA and AEA were measured as pure liquids. The number of scans per sample was 64 and the resolution 2.0 cm^{-1}. Photon correlation spectroscopy (PCS) measurements were performed using a BI-9000 Brookhaven light scattering apparatus (Brookhaven Instrument Cooperation), fitted with a 20 mW HeNe laser and the detector was set at a scattering angle of 90^{o}. The extent of particle swelling was characterised in terms of the particle volume swelling ratio, Q_p. SEM images were obtained using a Philips XL30 FEG-SEM with an accelerating voltage of 5kV. Samples were dried onto glass slides and coated with Au/Pd.

$$Q_v = \left(\frac{d_h}{d_{h(coll)}}\right)^3 \quad (1)$$

For equation (1) the parameters d_h and $d_{h(coll)}$ are the hydrodynamic diameters measured in the swollen and collapsed states, respectively. SEM measurements were obtained using a Philips FEGSEM instrument. A Malvern Zetasizer was used to measure the electrophoretic mobilities of the particles in the presence of aqueous 0.001 M $NaNO_3$. The mobilities were converted to zeta potentials (ζ) using the Smoluchowski equation[38].

RESULTS AND DISCUSSION

Microgel Composition

The microgel compositions were characterised using elemental analysis and FTIR. The experimental ratio of the % nitrogen to % carbon values ($R_{NC(exp)}$) was a useful gauge for the extent of PA inclusion (for PX-PA) or AEA functionalisation (for PX-PA-AEA). Because AEA is nitrogen rich, its inclusion within PX-PA-AEA should increase $R_{NC(exp)}$ for each system (Scheme 1). (All the elemental data obtained appear in Table S2.) Fig. 1 and Table 1 show the values for $R_{NC(exp)}$ for each microgel. Compared to the respective $R_{NC(exp)}$ values for PVP and PNP, those for PVP-PA and PNP-PA decreased because PA does not contain nitrogen. (PEA-PA and PEA monomers did not contain nitrogen.) Moreover, the $R_{NC(exp)}$ value increased upon AEA functionalisation for each microgel (Fig. 1). The increase of $R_{NC(exp)}$ was strongest for PEA-PA-AEA. These data qualitatively support the view that (a) PA was incorporated within the PX-PA microgels as a consequence of emulsion polymerisation and (b) AEA was subsequently incorporated into the PX-PA microgels (to give PX-PA-AEA) as a result of CuAAC.

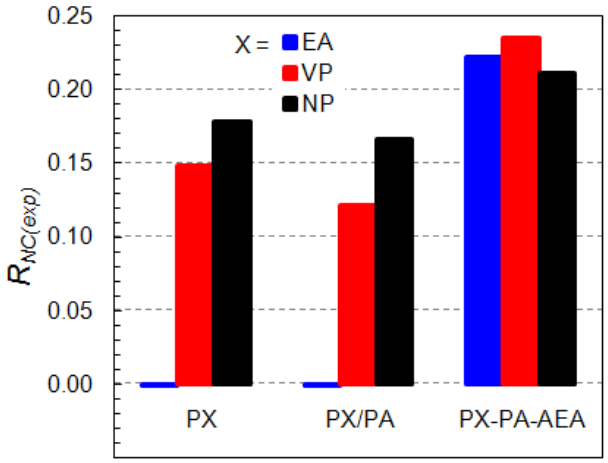

Fig. 1. Changes in composition for the microgels. The values for $R_{NC(exp)}$ (= %N/%C) decreased or increased, respectively, for incorporation of PA or AEA for the microgels based on VP and NP. The $R_{NC(exp)}$ values were zero for PEA and PEA-PA because PEA and PA did not contain nitrogen. *(Colour reproduction on web, B & W in print.)*

The values for $R_{NC(exp)}$ were used to calculate the compositions of the microgels. A description of the method used is given in the Supporting information. For PNP-PA and PVP-PA the compositions were determined from elemental analysis data (Table S2). For the PEA-PA microgel a nominal composition of PEA-$PA_{0.28}$ based on the masses of co-monomers used for preparation was assumed (Table 1). This appears to have been a good assumption 100% inclusion of AEA (i.e., PNP-PA-$AEA_{0.28}$) was determined - see Supplementary Information. Furthermore, quantitative inclusion of AEA into the other two microgels was apparent from the respective analyses. Our analyses did not consider competing reactions involving PA, such as crosslinking (discussed below). However, the extent of PA crosslinking seems to have been relatively low compared to the total PA contents because quantitative AEA inclusion was determined. We note that less than 1 mol.% of crosslinks can strongly restrict microgel swelling[2]. PA crosslinking is considered further below. All microgel compositions are shown in Table 1. We conclude that the AEA incorporation within PX-PA-AEA particles was determined by the PA content. This is consistent with the high efficiency reported for CuAAC click reactions[20, 21, 27].

Table 1. Characterisation data for the microgels.

Code	Composition[a]	$R_{NC(exp)}$	d_{SEM} / nm	d_h / nm in DMF	d_h / nm in water[b]	Q_p in DMF	Q_p in water	ζ / mV[c]
PEA	PEA	0	107 [16]	213 ± 11	102 ± 5	9.1 ± 1.4	1.0 ± 0.15	17.1
PEA-PA	PEA-$PA_{0.28}$[d]	0	125 [12]	157 ± 8	133 ± 7	1.6 ± 0.2	1.0 ± 0.15	12.9
PEA-PA-AEA	PEA-$(PA\text{-}EA)_{0.28}$	0.222	166 [10]	-	160 ± 8	-	1.7 ± 0.3[e]	23.6
PVP	PVP	0.148	372 [24]	664 ± 33	1225 ± 61[f]	4.5 ± 0.7	28 ± 4	18.8
PVP-PA	PVP-$PA_{0.18}$	0.121	339 [11]	512 ± 26	537 ± 27[f]	2.8 ± 0.4	3.3 ± 0.5[g]	20.4
PVP-PA-AEA	PVP-$(PA\_AEA)_{0.18}$	0.235	403 [24]	-	1020 ± 51[f]	-	23 ± 3[g]	20.6
PNP	PNP	0.178	245 [7.5]	417 ± 21	338 ± 17	37 ± 6[h]	20 ± 3[h]	0.2
PNP-PA	PNP-$PA_{0.063}$	0.166	200 [7.6]	505 ± 25	333 ± 17	18 ± 3[h]	5.1 ± 0.8[h]	6.8
PNP-PA-AEA	PNP-$(PA\text{-}AEA)_{0.063}$	0.211	249 [7.8]	-	375 ± 19	-	7.7 ± 1[h]	10.8

[a] The compositions were calculated from the $R_{NC(exp)}$ values unless otherwise stated – see Supplementary Information for method used. [b] Values measured at pH = 4. [c] Zeta potential measured at pH = 4. [d] Compositions assumed based on conditions used for preparation. [e] Estimated using the PEA-PA d_h value for collapsed diameter. [f] Measured at pH = 2. [g] Calculated using d_h values measured at pH = 2.0 and 12.0. [h] Estimated at pH = 4. For these calculations the hydrodynamic diameter for each respective microgel measured at 50 °C was used as the collapsed diameter.

The compositions for PX-PA (Table 1) show that PA incorporation decreased in the order PEA > PVP > PNP. This trend was unexpected. To the best of our knowledge the Alfrey and Price *Q* and *E* values (which are measures of reactivity and polarity, respectively[35]) for PA have not been reported. However, butyl acrylate has a similar structure to PA. The *Q* and *E* values for butyl acrylate (0.40 and 0.35[35]) and NP (0.40 and 0.47[39]) are very similar implying similar reactivity ratios and a statistical copolymer would be expected if all other factors were equal. It follows that differences in co-monomer reactivity ratios are not responsible for the low inclusion of PA within the PNP-PA microgel. A different explanation is required to account for the compositions in Table 1.

Swelling of primary particles by monomer is an important part of incorporation of co-monomers by emulsion polymerisation[40]. We tested the solubility of the *linear* polymers PNP_L, PVP_L and PEA_L in PA. It was found that PEA_L was readily soluble in PA. For PVP_L, the polymer also dissolved in PA, although this was slower than for PEA_L. Interestingly, PNP_L was insoluble in PA. We propose that the reason for the low PA incorporation within PNP microgels (and hence compositional difference) is incompatibility between PNP and PA. PA would not have been able to swell PNP-

rich particles during growth. This contrasts to PEA where good solubility of PA enhanced swelling of the PEA particles and incorporation. The less facile dissolution of PVP_L in PA is also consistent with the differences in PA incorporation evident (Table 1).

FTIR spectra for the microgels are shown in Fig. 2. The PEA-PA and PEA-PA-AEA microgels contained the highest PA and AEA contents based on elemental analysis data (28 mol.%, Table 1). The alkyne band at[31] 3280 cm^{-1} is clearly evident in the spectrum for PEA-PA (Fig. 2(a)) supporting a high extent of PA incorporation. The alkyne band, which was clearly evident in the spectrum for PA, was not apparent in the spectrum for PEA-PA-AEA, i.e., after CuAAC reaction of PEA-PA with AEA. Furthermore, the azide band (2100 cm^{-1}) from AEA (Fig. 2(a)) was not present in the spectrum for PEA-PA-AEA. These spectral changes for PEA-PA-AEA are indicative of a successful CuAAC reaction[29]. There is also evidence of a broad RNH_2 band[15, 41] at about 1590 cm^{-1}. This feature is also present in the FTIR spectrum for AEA. It can also be seen that the broadening of the features in the 3300 cm^{-1} region of the FTIR for PEA-PA-AEA match those of AEA and are absent from the spectrum for PEA-PA. The latter is also indicative of RNH_2[41-43]. Consequently, the FTIR spectra confirm that primary amine groups were incorporated (Scheme 1(a)) and are in qualitative agreement with the compositions for the EA-based microgels given in Table 1.

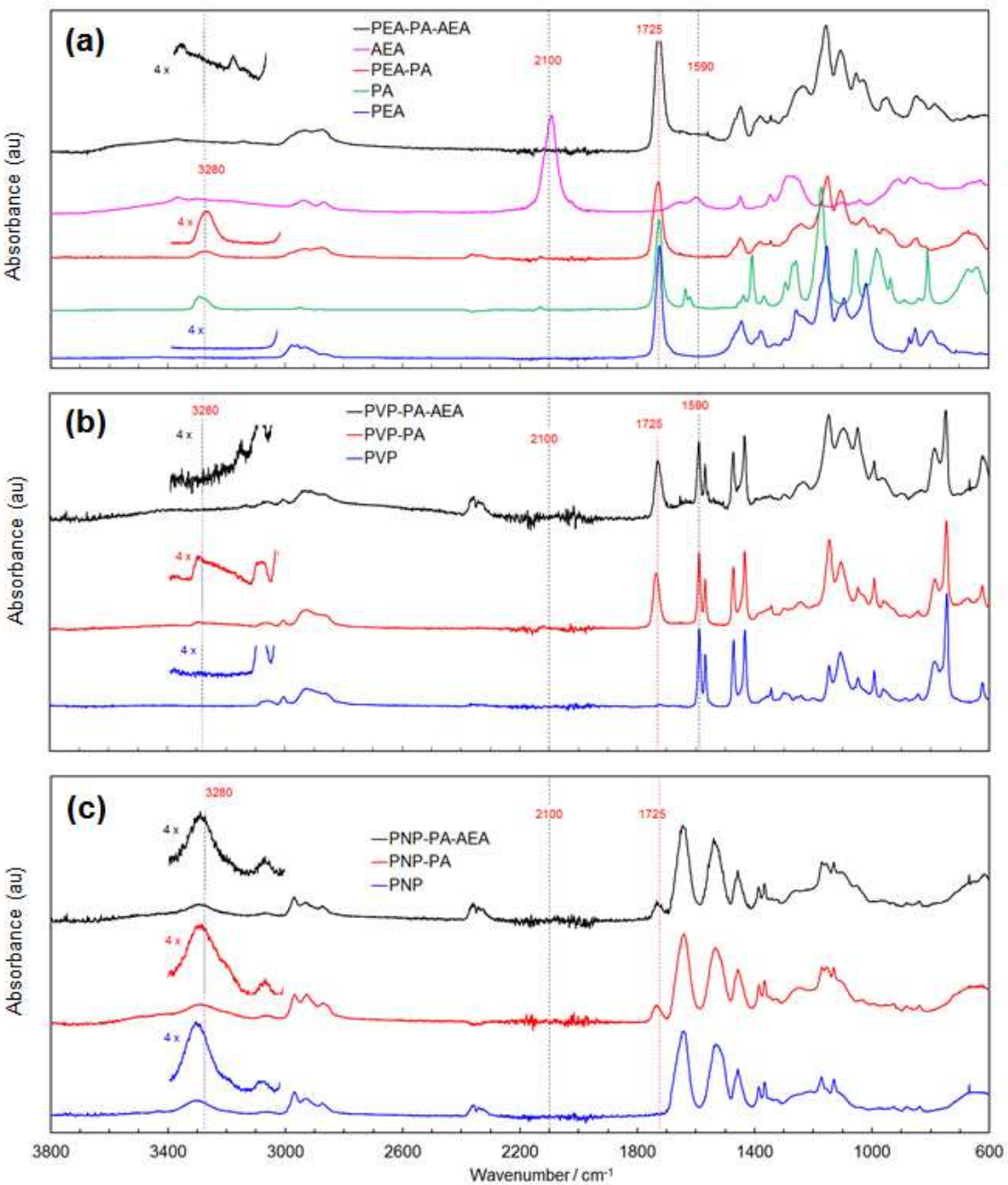

Fig. 2. FTIR spectra of various microgels. Spectra for AEA and PA are also shown in (a) for comparisons. Expanded spectra for the 3000 – 3400 cm^{-1} region are shown for the microgels. *(Colour reproduction on web, B & W in print.)*

The spectrum for PNP-PA (Fig. 2(b)) shows a weak alkyne band at 3280 cm^{-1}, which is consistent with the lower extent of incorporation (18 mol.%) compared to that for PEA-PA (28 mol.%). The band was superimposed on a broad RNH_2 band. For this microgel support for incorporation of PA can be found from the strong band due to the ester groups present at 1725 cm^{-1}. The latter band was not present in the spectrum for PVP. The band was also present in the spectrum for PVP-PA-AEA (Fig. 2(b)). The absence of the alkyne and azide bands in the spectrum for PVP-PA-AEA confirm

that efficient CuAAC reaction occurred. There is also evidence of a broad band at about 1590 cm^{-1} due to RNH_2 with sharper bands due to PVP superimposed on it. Furthermore, the broad absorption due to RNH_2 groups is also present in the spectrum in the 3300 cm^{-1} region. The spectrum for PVP-PA-AEA is also consistent with significant primary amine group incorporation.

Fig. 2(c) shows the spectra for the PNP microgel systems. For PNP-PA the alkyne band was obscured by a broad band due to N-H groups at about 3300 cm^{-1}. However, the ester band at 1725 cm^{-1} was clearly present; although, at a lower relative absorbance compared to the same band in the spectrum for PVP-PA (Fig. 2(b)). This confirms a lower PA incorporation within this microgel (6.3 mol.%). The spectrum for PNP-PA-AEA does not show evidence of an azide band, as expected. However, the FTIR spectrum does not show any clear RNH_2 bands because of the strong amide I band[44] in the 1650 cm^{-1} region and low AEA content.

The FTIR spectra for all of the microgels are consistent with the compositions determined from elemental analysis (Table 1). The CuAAC reactions for each of the microgels shown in Scheme 1 was quantitative. This shows that our simple approach to functionalise the microgels using CuAAC is generally applicable and only limited by the ability to incorporate PA into the PX-PA microgel particles during particle growth.

Microgel particle characterisation and swelling

SEM images for the microgels are shown in Fig. 3. The particles were well dispersed in each case as evidenced by separated particles. There was some evidence of a nodular surface morphology for the PX-PA and PX-PA-AEA (X = EA and VP) particles. The number-average diameters measured from SEM (d_{SEM}) for the PEA-based microgels were all close to the respective d_h values measured in water (Table 1), showing that the particles existed as isolated particles in dispersion. For the PVP-based microgels the d_{SEM} values are in the range of 339 to 403 nm and are in the same range as the d_h values measured for these microgels in water at pH = 12 (Fig. 4(c)), i.e., in the collapsed state. This also supports the view that the particles were well dispersed. A comparison between the

d_{SEM} and d_h values for the PNP-based microgels is more difficult because PNP microgels are well known to deform greatly upon deposition onto SEM stubs[45]. Values for d_h at 50 ^{o}C were measured (Fig. 6) and the values for PNP-PA and PNP-PA-AEA were about 195 nm. The latter value is close to the respective d_{SEM} values and confirms that particles existed as isolated particles in dispersion. Thus, the data strongly support the view that our CuAAC method (Scheme 1) did not result in significant aggregation, which is essential for a microgel functionalisation strategy to be useful.

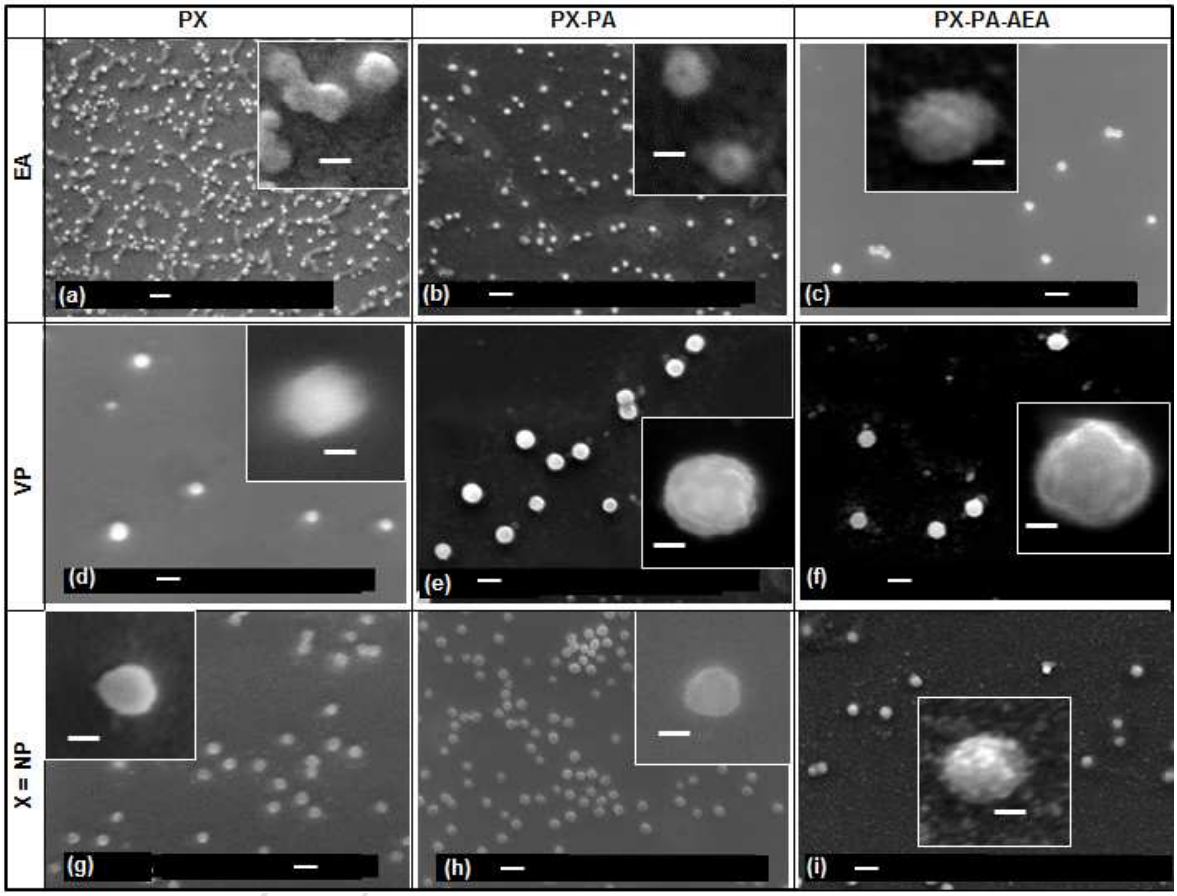

Fig. 3. SEM images for various microgel particles. The scale bars for the main images and insets represent 500 and 100 nm, respectively.

The high CuAAC efficiencies for the microgels established above imply complete access of the click reagents (PMDETA, CuBr and AEA) to all of the PA within the PX-PA particles. This implies that the microgel particles were swollen. We selected DMF as the dispersion solvent for the click reactions because (a) it has been used for CuAAC of AEA[22], (b) it was miscible with water and (c) the PX-PA microgel particles were swollen by that solvent. The latter is evident from the d_h values for PEA-PA, PNP-PA and PVP-PA measured in DMF (Table 1). It can be seen that the d_h values

for PEA-PA and PNP-PA dispersed in DMF were larger than the respective values measured in water. This could be seen visually for the PEA-PA dispersions in water and DMF at the same particle concentration (See Scheme 1(a)) where the turbidity was less for the DMF dispersion – due to swollen particles scattering less light. In the case of PVP-PA the d_h value of 512 nm measured for the particles in DMF (Table 1) was much higher than the collapsed value in water at pH = 12 (of 362 nm from Fig. 4(c)) and those microgel particles were also swollen in DMF.

A noticeable consequence of incorporating PA into the microgels was that the extent of particle swelling decreased. This can be seen from comparing the Q_p values for the PX or PX-PA (X = EA and NP) particles in DMF (Table 1). In each case the Q_p values were less for the PX-PA particles. The Q_p values for the PNP and PNP-PA microgels also follow this trend. However, those values are approximate because the diameters measured for each respectively microgel at 50 ^{o}C was used for $d_{h(coll)}$ in equation (1). PNP is known to retain water at 50 ^{o}C[46, 47]. Indeed, Destribats et al.[48] assumed that their PNP microgels contained 29 wt.% of water at 50 ^{o}C. This means that the true Q_p values will be larger than those shown in Table 1. The Q_p values used here for those systems are minimum values. Nevertheless, our comparison of the Q_p values calculated in this way within the PNP microgel series (PNP, PNP-PA and PNP-PA-AEA) is valid because the relatively low levels of PA and PA-AEA incorporated (ca. 6.3 mol.%) are unlikely to have significantly altered the water contents at 50 ^{o}C.

PA is soluble in DMF which suggests that the decreased swelling for the microgels containing PA discussed above is not due to PA-solvent incompatibility. PA is known to act as a crosslinking during emulsion polymerisation[30]. Accordingly, the decreased swelling for the PX-PA particles is attributed to crosslinking by PA units during particle formation. This is supported by a comparison of the Q_p values measured in DMF (Table 1) for PEA (9.1 ± 1.4) and PEA-PA microgel (1.6 ± 0.2). We tested this further by preparing a PEA-PA microgel without any added BDD crosslinker, i.e., BDD-free PEA-PA. The hydrodynamic diameters for the latter particles in water and DMF were, respectively, 144 ± 7 and 163 ± 8 nm. The value for Q_p was 1.5 ± 0.2. This Q_p value is not

significantly different to the value obtained for PEA-PA microgels prepared using BDD (Table 1). This result demonstrates that the crosslinking for the PEA-PA microgels prepared using BDD was dominated by PA. It follows that PA can be used to generate highly functionalised microgels where PA has two roles, i.e., as a crosslinker and a CuAAC site. This is a new observation for microgels.

It is instructive to compare the Q_p values for the PX-PA-AEA microgels at pH = 4 to those for the parent PX-PA microgels. The Q_p values increased in each case due to inclusion of AEA. Given the pK_a of primary amines should be about[49] 10 we can conclude that the increase in Q_p is because of electrostatic repulsion between neighbouring AEA groups within the microgel particles. The ζ values in Table 1 support this view because at low pH the values were highest for the PX-PA-AEA microgels. These data support primary amine group incorporation within PX-PA-AEA.

pH-dependent microgel particle properties

The trends for the d_h values described above at pH = 4 were maintained for the PEA-based microgels across the entire pH range (Fig. 4(a) and (b)). The Q_p values for the PEA-PA-AEA microgel particles in the pH range of 4 to 10 had an average value of 1.7 which is not significantly different to the Q_p value for the PEA-PA particles dispersed in DMF (1.6, Table 1). Although repulsion between RNH_3^+ groups was able to swell the particles in water, the maximum Q_p values are much lower than would normally be expected for microgel particles containing 28 mol.% of charged groups. For example anionic EA-based microgels containing about 30 mol.% of deprotonated $RCOO^-$ groups had Q_p values of around[50] 30. It is likely that PA crosslinks contribute to the strongly restricted swelling for PEA-PA-AEA. There was some evidence of a decrease in d_h (and Q_p) at a pH value of 12 (Fig. 4(a) and (b)), which would be expected due to deprotonation of the primary amine groups. However, complete collapse of the particles at a pH of 12 is not expected because the nitrogen-rich structure of AEA is hydrophilic.

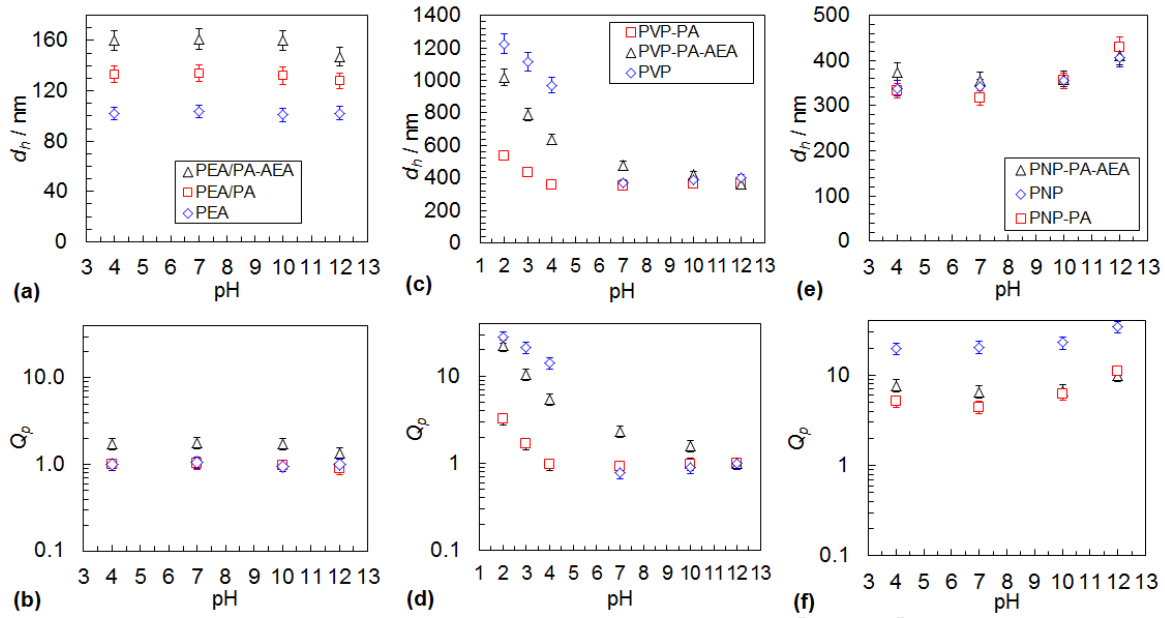

Fig. 4 pH-dependent swelling for various microgels. The figures on the top and bottom rows show the variations of hydrodynamic diameter and swelling ratio, respectively. In some cases the error bars are smaller than the symbols. The legends are the same for (a) and (b), (c) and (d) as well as (e) and (f). *(Colour reproduction on web, B & W in print.)*

The PVP-PA and PVP-PA-AEA microgels contained lower PA and PA-AEA contents (cf. PEA-PA and PEA-PA-AEA). They also contained high proportions of a pH-responsive monomer (VP). PVP has a pK_a of about[10] 4.9. The PVP microgel showed strong pH-triggered swelling (Fig. 4(c) and (d)) when the pH decreased to 4 or less, and the data are consistent with previous reports[10]. Importantly, the PVP-PA microgel showed a much lower swelling response (cf. PVP) which is attributed to the relatively high PA content (18 mol.%). Interestingly, after functionalisation with AEA the strong low pH swelling behaviour of PVP-PA-AEA returned and was comparable to that for the parent PVP particles. However, there was also evidence of increased swelling at pH = 7 and 10. We speculate that this ability to restore the original particle swelling behaviour is due to a relatively low level of additional crosslinking provided by the PA groups (cf. PEA-PA). The suppressed swelling for PVP-PA compared to PVP at low pH would have been the result of a dilution of the positive charged groups with non-charged PA. The loss of positive charge was restored upon functionalisation of the PA groups with AEA. This interpretation is supported by the higher Q_p values for PVP-PA-AEA at pH = 4 to 10 (Fig. 4(d)) compared to PVP-PA. However, the swelling from the AEA groups alone was not sufficient to strongly swell the PVP-PA-AEA particles at pH

values greater than the pK_a of PVP (ca. 4.9 for linear PVP[10]). This is probably due to the hydrophobicity of the non-charged VP units that opposed particle swelling in that pH range.

The variable pH data for the PNP, PNP-PA and PNP-PA-AEA microgels (Fig. 4(e) and (f)) were different to the other systems because there were few differences between the three microgels for this series. This is attributed to the content of PA and PA-AEA being the lowest of the three microgel systems (6.3 mol.%). However, the d_h and Q_p values at pH = 4 and 7 were higher for PNP-PA-AEA compared to PNP-PA, supporting the view that electrostatic swelling occurred. Surprisingly there was a significant increase in swelling at pH = 12 for all three microgels. This is proposed to be due to hydrolysis and is discussed further below.

The effect of pH on the ζ values were also measured (Fig. 5). For all three microgel systems there was a strong pH dependence of ζ with its value being highest at low pH. Moreover, the ζ values at pH = 4 and 7 for all of the PX-PA-AEA microgels were significantly larger than those for the respective PX-PA microgels. This suggests that there was a higher positive charge density for the AEA-containing microgels in that pH range. This finding suggests that each of the PX-PA-AEA microgels had comparable outer shell structures which contained primary amine groups. However, it is also possible that protonated 1,2,3-triazole species also contributed to the positive charge in the above pH range because these species are known to have a pK_a around[51] 9.

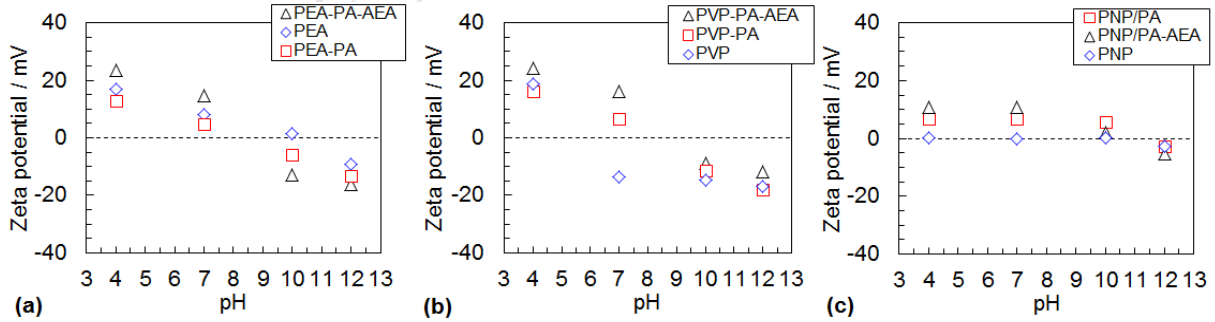

Fig. 5 pH-dependent zeta potentials for various microgels. In all cases the error bars are smaller than the symbols. *(Colour reproduction on web, B & W in print.)*

An important observation concerning the ζ data is that relative changes for these values did not always match the respective changes for d_h. For example, the ζ values for PVP-PA and PVP/PEA-

AEA (Fig. 4(b)) show similar strong decreases with increasing pH and have comparable values. However, the changes in d_h (and Q_p) for PVP-PA-AEA are more pronounced than those for PVP-PA (Fig. 4(c) and (d)). This is because ζ and d_h values measure outer layer and whole particle properties, respectively. The charge density changes that occur within outer layer of microgels do not always map onto changes in charge density occurring within the particle interior[11]. We consider the ζ values as a guide to the changes in swelling and charge densities that occur in the outer shell of the microgel particles or surface of the microgels in the collapsed, latex, form.

The ζ data for all of the systems show an isoelectric point (iep). The PEGMa provided steric stabilisation and prevented aggregation of these dispersions even when the pH passed through the ieps. The ieps indicate that negatively charged species were present. Amidines have a pK_a in the vicinity of[52] 7. Furthermore, they are known to undergo hydrolysis, along with esters, under alkaline conditions. This is a common explanation for the appearance of ieps within amidine-stabilised latexes and microgels[52, 53]. It is the acquisition of negative charge in the shell of the PNP-based microgels that may explain the moderate swelling observed for these microgels at pH = 12 (Fig. 4(e) and (f)). We note that there was no evidence of aggregation for any of these dispersions.

To further probe the effect of incorporating PA and PA-AEA within the PNP microgels variable temperature d_h and ζ measurements were conducted (Fig. 6). The data show that the similarity of the hydrodynamic diameters for PEA-PA and PEA-PA-AEA remained over the entire temperature range studied (25 – 50 ^{o}C). By contrast, the particle size changes were much higher for PNP. This can be seen from Fig. S2 where Q_p values are plotted as a function of temperature. This is further support that PA acted as a crosslinker. PA is hydrophobic and would be expected to suppress swelling and this would have contributed to the low Q_p values. However, the fact that there was only a small increase in Q_p occurred upon AEA incorporation suggests that the primary cause for lack of swelling was the covalent crosslinking involving PA.

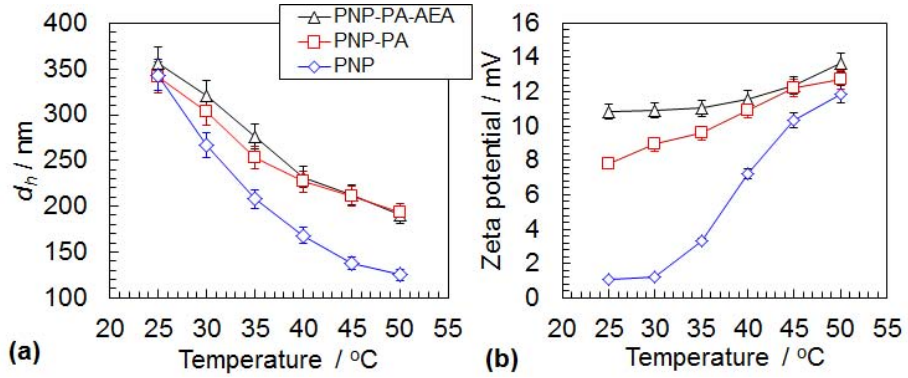

Fig. 6. Variable temperature diameter (a) and zeta potential data (b) for NP-based microgels. The data were obtained at pH = 7. *(Colour reproduction on web, B & W in print.)*

The variable temperature ζ data (Fig. 6(b)) show clear differences between the three PNP-based microgel systems. The ζ values at temperatures of 25 – 35 °C increased in the order PNP < PNP-PA < PNP-PA-AEA. This implies that there were significant differences in the volume surface charge density in the outer layer of these particles. The charge density was highest for PNP-PA-AEA. The ζ values were similar at 50 °C because the particles were mostly collapsed and had similar surface charge densities. These three microgels would be expected to have possessed similar charge densities when prepared because they were prepared using similar monomer-to-initiator ratios.

A final point can be made from a comparison of the d_h and ζ data (Fig. 6) for PNP-PA and PNP-PA-AEA. The equivalence of the d_h data for these two microgels and the dissimilarity of the ζ data at lower temperatures, coupled with the relatively low levels for their incorporation (6.3 mol.%), imply that the PA and PA-AEA groups were preferentially located in the outer shell of the microgels. This is potentially useful for future microgel functionalisation using CuAAC chemistry because it facilitates their accessibility to reactants.

CONCLUSIONS

In this study we have investigated the ability to functionalise three different types of microgels with primary amine groups using CuAAC chemistry. Incorporation of AEA into the microgels was quantitative for each microgel system which confirms the principle of achieving high yield CuAAC reactions applies to swollen microgel particles. The limiting factor controlling AEA incorporation

was the PA content in the precursor microgel particles. The highest AEA content incorporated was for PEA-PA-AEA which contained 28 mol.% of AEA. Using this approach we prepared three new examples of microgels containing primary amine groups; PX-PA-AEA (X = EA, VP and NP). The extent of incorporation of AEA into PNP-PA-AEA was the lowest (6.3 mol.%) and this was attributed to the inability of PA to swell PNP. The PCS and zeta potential data for that system imply that the PA-AEA units were located mostly in the outer shell of the PNP/microgel-AEA particles. PA was found to act as a crosslinker and it was possible to use that co-monomer as the only crosslinker for PEA microgel preparation. All of the PX-PA-AEA microgels exhibited pH-triggered swelling in water due to the primary amine groups at pH values less than or equal to 7. The pH-responsive swelling was strongest for PVP-PA-AEA and this system appeared to provide a good compromise between crosslinking due to PA and swelling by AEA incorporation. This study has established a general method that can be used to efficiently functionalise microgels with azide-containing molecules by CuAAC. Our CuAAC method for microgels did not cause aggregation and appears versatile. In addition, the three new PX-PA-AEA microgels (X = EA, VP and NP) studied here offer additional functionalisation opportunities through the wide range of reactions available for primary amines[14].

Acknowledgements

BRS and RF would like to thank the EPSRC for funding.

References

1. L. Hu, A. K. Sarker, M. R. Islam, X. Li, Z. Lu, and M. J. Serpe. *J. Polym. Sci. , A; Polym. Chem.* 2013, **51**, 3004.
2. B. R. Saunders, N. Laajam, E. Daly, S. Teow, X. Hu, and R. Stepto. *Adv. Coll. Interf. Sci.* 2009, **147-148**, 251.
3. N. M. B. Smeets, and T. Hoare. *J. Polym. Sci. , A; Polym. Chem.* 2013, **51**, 3027.
4. A. Fernandez-Barbero, I. J. Suarez, B. Sierra-Martin, A. Fernandez-Nieves, F. J. de las Nieves, M. Marquez, J. Rubio-Retama, and E. Lopez-Cabarcos. *Adv. Coll. Interf. Sci.* 2009, **147-148**, 88.
5. R. Pelton. *Adv. Coll. Interf. Sci.* 2000, **85**, 1.
6. P. A. FitzGerald, D. Dupin, S. P. Armes, and E. J. Wanless. *Soft Matter* 2007, **3**, 580.
7. J. D. Debord, and L. A. Lyon. *Langmuir* 2003, **19**, 7662.
8. S. Fujii, and S. P. Armes. *Langmuir* 2006, **22**, 6818.
9. Y. Wang, J. Nie, B. Chang, Y. Sun, and W. Yang. *Biomacromolecules* 2013, **14**, 3034.
10. D. Dupin, S. Fujii, S. P. Armes, P. Reeve, and S. M. Baxter. *Langmuir* 2006, **22**, 3381.
11. H. Dalmont, O. Pinprayoon, and B. R. Saunders. *Langmuir* 2008, **24**, 2834.
12. D. Klinger, and K. Landfester. *Macromolecules* 2011, **44**, 9758.
13. A. H. Milani, T. J. Freemont, J. A. Hoyland, D. J. Adlam, and B. R. Saunders. *Biomacromolecules* 2012, **13**, 2793.
14. R. K. Pinschmidt. *J. Polym. Sci. A., Polym. Chem.* 2010, **48**, 2257.
15. S. Thaiboonrod, C. Berkland, A. H. Milani, R. Ulijn, and B. R. Saunders. *Soft Matter* 2013, **9**, 3920.
16. Z. P. Demko, and K. B. Sharpless. *Angew. Chem. Int. Ed.* 2002, **41**, 2110.
17. Z. P. Demko, and K. B. Sharpless. *Angew. Chem. Int. Ed.* 2002, **41**, 2113.
18. N.-T. Huynh, Y.-S. Jeon, M. Zrinyi, and J.-H. Kim. *Polym. Int.* 2013, **62**, 266.
19. X. Jiang, E. B. Vogel, M. R. Smith III, and G. L. Baker. *Macromolecules* 2008, **41**, 1937.
20. W. H. Binder, and R. Sachsenhofer. *Macromol. Rapid Commun.* 2007, **28**, 15.
21. R. K. Iha, K. L. Wooley, A. M. Nystrom, D. J. Burke, M. J. Kade, and C. J. Hawker. *Chem. Rev.* 2009, **109**, 5620.
22. S.-H. Jung, H.-Y. Song, Y. Lee, H. M. Jeong, and H. Lee. *Macromolecules* 2011, **44**, 1628.
23. J. Budhathoki-Uperty, J. F. Reuther, and B. M. Novak. *Macromolecules* 2012, **45**, 8155.
24. H. Nulwala, D. J. Burke, A. Khan, A. Serrano, and C. J. Hawker. *Macromolecules* 2010, **43**, 5474.
25. X. Liu, H.-N. Zheng, Y.-Z. Ma, Y.-Z. Ma, Q. Yan, and S.-J. Xiao. *J. Coll. Interf. Sci.* 2011, **358**, 116.
26. Y. Yu, C.-K. Chen, W.-C. Law, J. Mok, J. Zou, P. N. Prasad, and C. Cheng. *Mol. Pharmaceutics* 2013, **10**, 867.
27. H. C. Kolb, M. G. Finn, and K. B. Sharpless. *Angew. Chem. Int. Ed.* 2001, **40**, 2004.
28. N. Li, and W. H. Binder. *J. Mater. Chem.* 2011, **21**, 16717.
29. M. T. Gokmen, W. V. Camp, P. J. Colver, S. A. F. Bon, and F. E. Du Prez. *Macromolecules* 2009, **42**, 9289.
30. R. D. Roeder, P. Rungta, V. Tsyalkovskyy, Y. Bandera, and S. H. Foulger. *Soft Matter* 2012, **8**, 5493.
31. D. D. Evanoff, S. E. Hayes, Y. Ying, G. H. Shim, J. R. Lawrence, J. B. Carroll, R. D. Roeder, J. M. Houchins, C. F. Huebner, and S. H. Foulger. *Adv. Mater.* 2007, **19**, 3507.
32. R. K. O'Reilly, M. J. Joralemon, K. L. Wooley, and C. J. Hawker. *Chem. Mater.* 2005, **17**, 5976.
33. Z. Meng, G. R. Hendrickson, and L. A. Lyon. *Macromolecules* 2009, **42**, 7664.
34. S. G. Kupal, B. Cerroni, S. V. Ghugare, E. Chiessi, and G. Paradossi. *Biomacromolecules* 2012, **13**, 3592.
35. J. Brandrup, E. H. Immergut, E. A. Grulke, A. Abe, and D. R. Bloch (1999) *CRC Polymer Handbook*, 4 ed., John Wiley & Sons.
36. J. McParlane, D. Dupin, J. M. Saunders, S. Lally, S. P. Armes, and B. R. Saunders. *Soft Matter* 2012, **8**, 6239.
37. H. G. Schild, and D. A. Tirrell. *Langmuir* 1991, **7**, 665.
38. D. J. Shaw. *Introduction to colloid and surface chemistry, Butterworth-Heinemann Ltd, Oxford* 1992.
39. C. K. Chiklis, and J. M. Grasshoff. *J. Polym. Sci. (A2)* 1970, **8**, 1617.
40. P. A. Lovell, and M. S. El-Aasser. *Emulsion polymerization and emulsion polymers, Wiley* 1997.

41. L. Shi, and C. Berkland. *Macromolecules* 2007, **40**, 4635.
42. R. C. Weast, M. J. Astle, and W. H. Beyer (1985) *CRC Handbook of Chemistry and Physics*, 65 ed., CRC, Boca Raton.
43. S. Seifert, F. Simon, G. Baumann, M. Hietschold, A. Seifert, and A. Spange. *Langmuir* 2011, **27**, 14279.
44. Y. Maeda, T. Higuchi, and I. Ikeda. *Langmuir* 2000, **16**, 7503.
45. B. R. Saunders, and B. Vincent. *J. Chem. Soc., Faraday Trans.* 1996, **92**, 3385.
46. H. M. Crowther, and B. Vincent. *Coll. Polym. Sci.* 1998, **276**, 46.
47. A. K. Lele, M. M. Hirve, M. V. Badiger, and R. A. Mashelkar. *Macromolecules* 1997, **30**, 157.
48. M. Destribats, M. Wolfs, F. Pinaud, V. Lapeyre, E. Sellier, V. Schmitt, and V. Ravaine. *Langmuir* 2013, **29**, 12367.
49. K. Samaru, H. Matsuoka, and H. Yamaoka. *J. Phys. Chem.* 1996, **100**, 9000.
50. R. Liu, A. H. Milani, T. J. Freemont, and B. R. Saunders. *Soft Matter* 2011, **7**, 4696.
51. S. Granados-Focil, R. C. Woudenberg, O. Yavuzcetin, M. T. Tuominen, and E. B. Coughlin. *Macromolecules* 2007, **40**, 8708.
52. F. Meunier, A. Elaissari, and C. Pichot. *Polym. Adv. Tech.* 1994, **6**, 489.
53. F. Sauzedde, F. Ganachaud, A. Elaissari, and C. Pichot. *J. Appl. Polym. Sci.* 1997, **65**, 2331.

SUPPORTING INFORMATION

A general method for functionalisation of microgel particles with primary amines using click chemistry

Robert Farley[a] and Brian R. Saunders[a,*]

[a]*Biomaterials Research Group, Manchester Materials Science Centre, School of Materials, The University of Manchester, Grosvenor Street, Manchester, M1 7HS, U.K.*

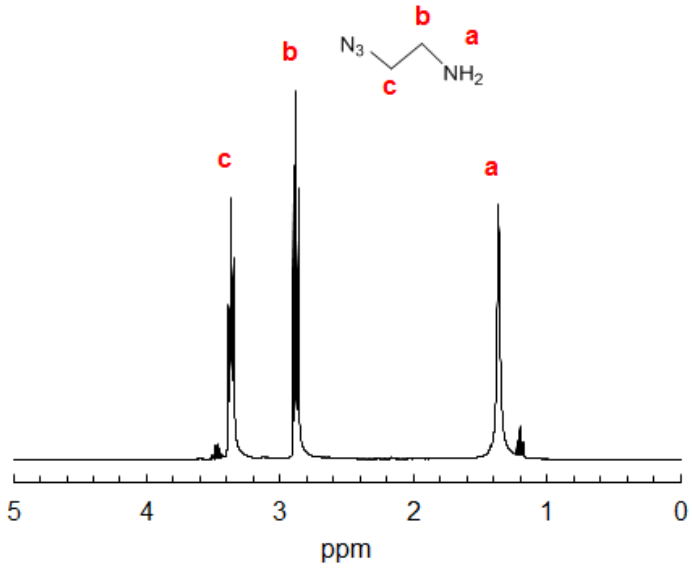

Fig. S1. ^{1}H NMR spectrum for AEA.

Table S1. Preparation and characterisation data for the microgels investigated in this work

PX or PX-PA	Nominal composition	X / g	Crosslinker[a] / g	PA / g
PEA	$PEA_{0.99}BDD_{0.01}$	14.37	0.29 (BDD)	0
PVP	$PVP_{0.99}DVB_{0.01}$	14.79	0.19 (DVB)	0
PNP	$PNP_{0.99}BA_{0.01}$	14.79	0.20 (BA)	0
PEA-PA	$PEA_{071}PA_{0.28}BDD_{0.01}$	10.35	0.15 (BDD)	4.50
PVP-PA	$PVP_{0.71}PA_{0.28}DVB_{0.01}$	10.54	0.096 (DVB)	4.36
PNP-PA	$PNP_{071}PA_{0.28}BA_{0.01}$	10.73	0.11 (BA)	4.13

[a] The identity of the crosslinker is shown in brackets.

Calculation of compositions for microgels using elemental analysis data

1. Introduction

In the following we assume for calculation purposes that the only contributions to % C, %N and R_{NC} (= %N/%C) values are the monomers shown in Scheme S1. The contributions from PEGMA, crosslinker and added surfactant are assessed empirically using the control (homopolymer) microgels (below). Our approach is described in the following where we first consider the PVP and PNP-based microgels before finishing with the PEA-based microgels. In the following calculations we ignore crosslinking of PA for the reasons discussed in the main text.

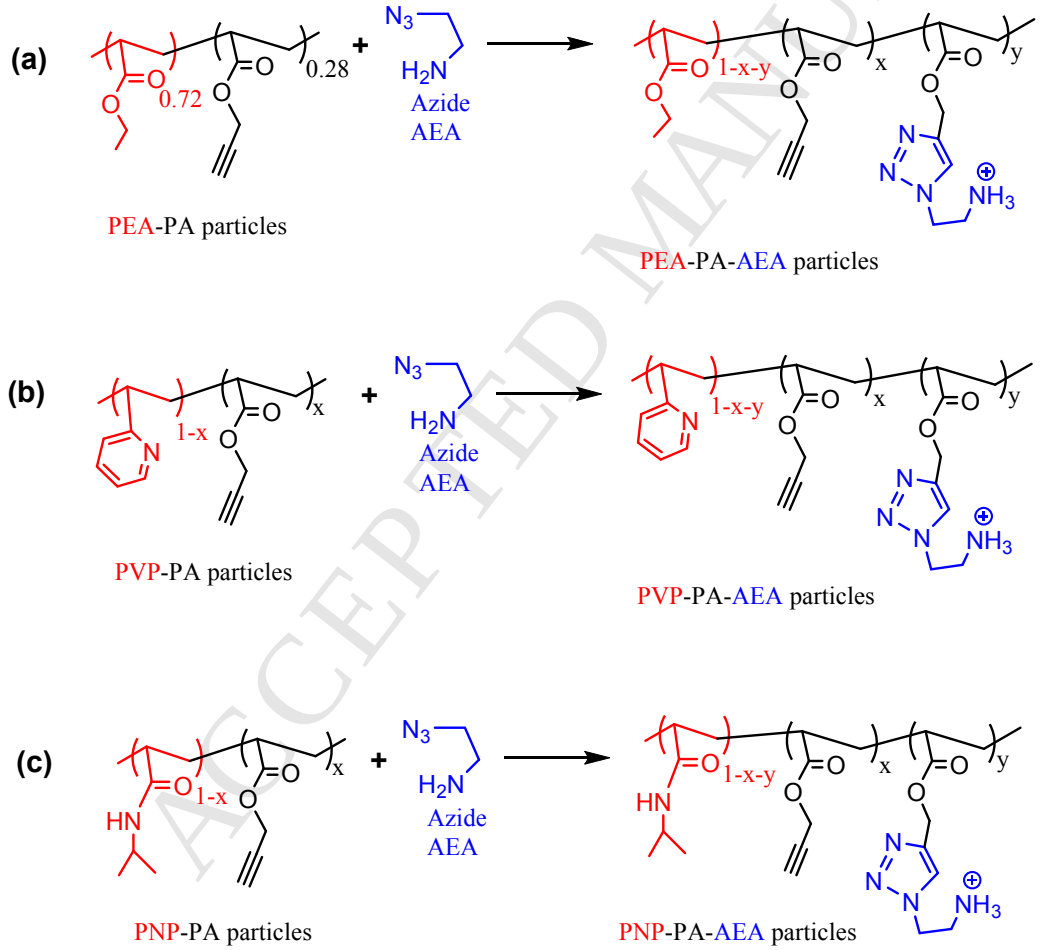

Scheme S1. CuAAC reaction schemes used to determine microgel compositions.

2. PVP-based microgels

Although we cannot be certain of the contributions of PEGMA and DVB to the experimental R_{NC}

value ($R_{NC(exp)}$), this can be estimated using the theoretical value ($R_{NC(thry)}$) for the PVP microgel as follows.

2.1 PVP microgel

The repeat unit formula for PVP is C_7H_7N with a molecular weight of *MW*. The value of $R_{NC(thry)}$ is:

$$R_{NC(thry)} = \frac{\left(\frac{1400.7 \; x \; 100}{MW}\right) x1}{\left(\frac{1201.1 \; x \; 100}{MW}\right) x7} = 0.167 \qquad \text{(S1)}$$

The value for $R_{NC(exp)}$ was 0.148. This difference is ascribed to incorporation of carbon-rich PEGMA and DVB. The difference was 0.019 from the following equation:

$$\Delta R_{NC} = R_{NC(thry)} - R_{NC(exp)} \qquad \text{(S2)}$$

We therefore added ΔR_{NC} to the $R_{NC(exp)}$ values for the PVP-PA and PVP-PA-AEA microgels in order to compensate for the decrease due to PEGMA and DVB incorporation. These corrected values ($R_{NC(exp)}^{Cor} = R_{NC(exp)} + \Delta R_{NC}$) are shown in Table S2.

Table S2. Elemental analysis data used for composition calculations[a]

Code	% C	% H	% N	$R_{NC(exp)}$	ΔR_{NC}	$R_{NC(exp)}^{Cor}$
PEA	58.77 ± 0.26	8.46 ± 0.26	0	0.000	0.0175	-
PEA-PA	59.48 ± 0.27	7.38 ± 0.23	0	0.000	0.0175	-
PEA-PA-AEA	51.20 ± 0.23	6.94 ± 0.22	11.39 ± 0.05	0.222 ± 0.001	0.0175	0.240
PVP	75.66 ± 0.34	7.63 ± 0.24	11.23 ± 0.05	0.148 ± 0.001	0.019	-
PVP-PA	73.33 ± 0.33	6.85 ± 0.21	8.90 ± 0.04	0.121 ± 0.001	0.019	0.140
PVP-PA-AEA	62.56 ± 0.28	7.05 ± 0.22	14.73 ± 0.07	0.235 ± 0.001	0.019	0.255
PNP	60.00 ± 0.27	9.97 ± 0.31	10.70 ± 0.05	0.178 ± 0.001	0.016	-
PNP-PA	61.00 ± 0.27	9.90 ± 0.31	10.13 ± 0.05	0.166 ± 0.001	0.016	0.182
PNP-PA-AEA	57.23 ± 0.26	8.78 ± 0.27	12.08 ± 0.06	0.211 ± 0.001	0.016	0.227

[a] See text for meanings of the parameters. The errors are estimated from multiple analyses for related polymers prepared in our laboratory and analysed by the same instrument and methods as used for the microgels studied here.

2.2 PVP-PA microgel

We next consider PVP-PA, which has a repeat unit formula of $(C_7H_7N)_{1-x}(C_6H_6O_2)_x$ from Scheme S1(b). The following equations apply.

$$\%C = \left(\frac{12.011\ x\ 100}{MW}\right)[7(1-x)+6x] \quad \text{(S3)}$$

$$\%N = \left(\frac{14.007\ x\ 100}{MW}\right)(7-x) \quad \text{(S4)}$$

Using these equations and the definition for R_{NC} (= %N/%C)), we obtained:

$$x = \frac{1.1662 - 7R_{NC}}{1.1662 - R_{NC}} \quad \text{(S5)}$$

Inserting the value of $R_{NC} = R_{NC(exp)}^{Cor} = 0.140$ into equation (S5) gives $x = 0.18$. The estimated composition of the microgel was PVP-$PA_{0.18}$. The latter does not show the crosslinker (DVB) because its nominal concentration was very small (1 mol.% with respect to total monomer used from Table S1). For this reason the crosslinker is not shown in the other estimated compositions.

2.3 PVP-PA-AEA microgel

PVP-PA-AEA has the structural formula (Scheme S1(b)) of $(C_7H_7N)_{1-x-y}(C_6H_6O_2)_x(C_8H_{12}N_4O_2)_y$. Using the constraint that $x + y = 0.18$, it can be shown that the following equation applies.

$$x = \frac{1.796 - 7.18R_{NC}}{4.6648 - 2R_{NC}} \quad \text{(S6)}$$

Inserting the value of $R_{NC} = R_{NC(exp)}^{Cor} = 0.255$ into equation (S6) gives $x = -0.008$, which is taken as $x = 0$, and hence, $y = 0.18$. The composition of this microgel was PVP-$(PA\text{-}AEA)_{0.18}$, i.e., 100% efficiency for the CuAAC reaction.

3. PNP-based microgels

We follow a similar approach to that described above for these microgels.

3.1 PNP microgel

The repeat unit formula for PNP is $C_6H_{11}NO$ with a molecular weight of *MW*. The value of $R_{NC(thry)}$ comes from:

$$R_{NC(thry)} = \frac{\left(\frac{1400.7\ x\ 100}{MW}\right)x1}{\left(\frac{1201.1\ x\ 100}{MW}\right)x6} = 0.194 \quad \text{(S7)}$$

The value for $R_{NC(exp)}$ was 0.178. The difference between these values (ΔR_{NC}) was 0.016 from equation (S2). This values was used to calculate $R_{NC(exp)}^{Cor}$ values for PNP-PA and PNP-PA-AEA (Table S2).

3.2 PNP-PA microgel

PNP-PA has a repeat unit formula of $(C_6H_{11}NO)_{1-x}(C_6H_6O_2)_x$ from Scheme S1(c). It can be shown that the following equation applies.

$$x = 1 - 5.145R_{NC} \quad \text{(S8)}$$

Inserting the value of $R_{NC} = R_{NC(exp)}^{Cor} = 0.182$ into equation (S8) gives $x = 0.063$. The composition of the microgel was PNP-$PA_{0.063}$.

3.3 PNP-PA-AEA microgel

PNP-PA-AEA has the structural formula (Scheme S1(c)) of $(C_6H_{11}NO)_{1-x-y}(C_6H_6O_2)_x(C_8H_{12}N_4O_2)_y$. Using the constraint that $x + y = 0.063$, then it can be shown that the following equation applies.

$$x - \frac{1.39 - 6.13R_{NC}}{4.66 - 2R_{NC}} \quad \text{(S9)}$$

Inserting the value of $R_{NC} = R_{NC(exp)}^{Cor} = 0.227$ into equation (S9) gives $x = -0.0004$, which is taken as $x = 0$ and hence, $y = 0.063$. The composition of this microgel was PNP-$(PA\text{-}AEA)_{0.063}$, i.e., 100% efficiency for the CuAAC reaction.

4. PEA-based microgels

We followed generally a similar approach to that above for these microgels.

4.1 PEA and PEA-PA microgels

The repeat unit formulae for PEA and PEA-PA are $C_5H_8O_2$ and $(C_5H_8O_2)_{1-x}(C_6H_6O_2)_x$, respectively (Scheme S1(a)). Because these systems did not contain nitrogen we could not determine a value for ΔR_{NC} from equation (S2) or calculate a value for x from R_{NC} values. A simplification was required. The structures for EA and PA are similar and furthermore PEA was soluble in PA. Furthermore, there was a relatively strong peak for the acetylene band at 3280 cm^{-1} in the FTIR spectrum for

PEA-PA (Fig. 2(a)). Therefore, we assume that complete PA incorporation occurred and that the composition was equivalent to that used for its preparation, i.e., PEA-$PA_{0.28}$.

4.2 PEA-PA-AEA microgel

PEA-PA-AEA has the structural formula (Scheme S1(a)) of $(C_5H_8O_2)_{1-x-y}(C_6H_6O_2)_x(C_8H_{12}N_4O_2)_y$. As explained in Section 4.1 we could not determine a value for ΔR_{NC}. We therefore used the average of the values for PVP and PNP. From Table S2, the ΔR_{NC} used was 0.0175.

Using the constraint that $x + y = 0.28$, then it can be shown that the following equation applies.

$$x = \frac{1.3061 - 5.84R_{NC}}{4.6648 - 2R_{NC}} \qquad \text{(S10)}$$

Inserting the value of $R_{NC} = R_{NC(exp)}^{Cor} = 0.240$ into equation (S10) gives $x = -0.023$, which is taken as $x = 0$ and hence, $y = 0.28$. The initial assumption that $x = 0.28$ for PEA-PA resulted in the composition of this microgel being estimated as PEA-$(PA\text{-}AEA)_{0.28}$, i.e., 100% efficiency for the CuAAC reaction. This supports the validity of the initial assumption of $x = 0.28$ for PEA-PA.

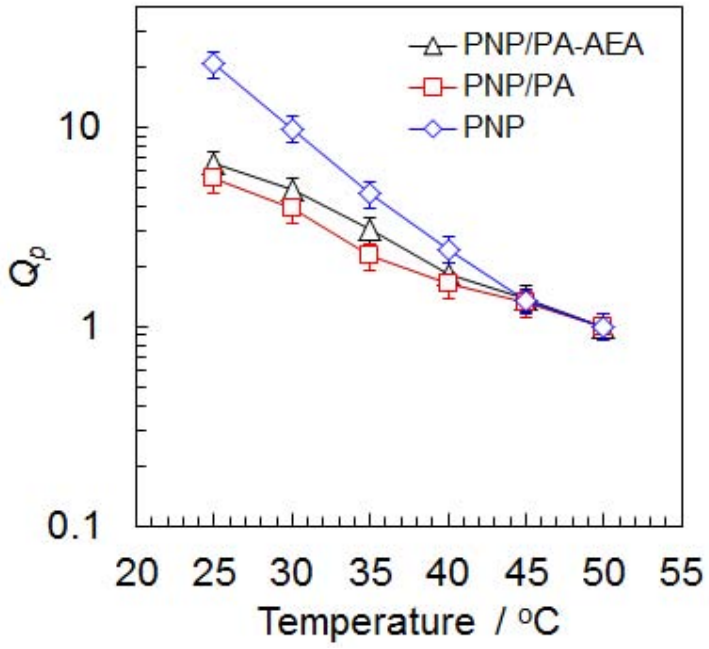

Fig. S2 Variation of estimated particle volume swelling ratio with temperature for PNP-based microgels. The measurements were obtained at pH = 7.